Excess Li$_2$O Additives to Promote Grain Boundary Growth and Improve Ionic Conductivity of LiTa$_2$PO$_8$ Solid Electrolytes

Qian Zhang[1,2]*, Fuhai Meng[2], Ruixiong Liao[2], Long Chen[2], Mengqian Xu[2], Shengwen Zhong[2], Jun Chen[2] and Anxian Lu[1]*

[1] School of Materials Science and Engineering, Central South University, Changsha, China, [2] Metallurgical Division of Materials Chemistry, Key Laboratory of Battery Power and Materials Jiangxi Province, Jiangxi University of Science and Technology, Ganzhou, China

LiTa$_2$PO$_8$ (LTPO) is a new solid-state lithium ion electrolyte material reported in the latest research, which has high bulk ionic conductivity and low grain boundary ion conductivity. However, it is difficult to density with conventional sintering methods. Herein, in this work, the solid-phase synthesis method was used to prepared the LTPO solid-state electrolyte, and the influence of the amount of lithium on the structure and performance of LTPO electrolyte material was investigated. The results show that the excess Li$_2$O does not increase other impurities and does not change the structure of the material, but the liquid phase produced by the excess Li$_2$O can promote the elimination of interfacial pores, accelerate the direct bonding of grains and improve the ionic conductivity of grain boundary, thus improving the overall ionic conductivity of the material. Considering the volatilization of lithium and the impact of liquid phase sintering at high temperatures and the content restructuring, after adding 20 wt% excess formulation of Li$_2$O, the resultant of LTPO density is 5.0 g/cm^3, the density reaches 85.58%. As a result, the total ionic conductivity of the electrolyte is 3.28 $\times$ 10^{-4} S/cm at 25°C, and the Li-ion diffusion activation energy is 0.27 eV. In addition, after loading this electrolyte into a Li–Li symmetric battery, it is proved that the electrolyte has lithium ion transport performance and can be used in all-solid-state batteries. However, it is also found from cyclic voltammetry (CV) and X-ray photoelectron spectroscopy (XPS) analysis that the interface between LTPO material and Li is unstable, and Ta^{5+} ions are reduced, which will be another key issue to be addressed in the future.

Keywords: solid oxide electrolyte, Li-ion conductor, interface impedance, Li-ion batteries, LiTa$_2$PO$_8$

INTRODUCTION

All-solid-state lithium batteries are non-flammable and can effectively improve the energy density and safety performance of lithium batteries, which has aroused widespread interest among researchers. However, its low ionic conductivity is the biggest obstacle to its application. The electrolyte is the key material of solid-state batteries, and the quality of electrolyte greatly affects the performance of solid-state batteries. The current solid electrolytes can be divided into organic

polymer type and inorganic type. Among them, the organic polymer electrolyte is composed of the polymer matrix [polyethylene oxide (PEO), polypropylene oxide (PPO), polymethacrylic acid (PMAA), methyl ester (PMMA), polyacrylonitrile (PAN), polyvinylidene fluoride (PVDF)] and lithium salts ($LiClO_4$, $LiPF_6$, and $LiBF_4$), in which the lithium salt is dissolved during the polymerization. In this case, a thin-film electrolyte material is constructed on the surface of collector (Long et al., 2016; Muench et al., 2016; Zhou et al., 2019). The ionic conductivity of the polymer electrolyte at room temperature is not high (10^{-5}–10^{-7} S/cm) and high operating temperature is required to be maintained between 60 and 80°C, which greatly limits the application of the organic polymer electrolyte (Zhou et al., 2019). Inorganic non-metal solid electrolytes have structures such as glass sulfide, garnet, NASICON, and perovskite. Among them, the ionic conductivity of glass sulfides is comparable to the liquid electrolyte, but the S element will react with water to produce toxic H_2S gas, its safety and stability need to be further improved (Kato et al., 2016). The garnet structure $Li_{6.6}La_3Zr_{1.6}Ta_{0.4}O_{12}$ with an ion conductivity of 1.18×10^{-3} S/cm at room temperature is synthesized by using spark plasma sintering (SPS) technology (Dong et al., 2019). This type of material has ionic conductivity close to that of commonly used lithium ion electrolytes, but it is unstable and easily reacts with moisture and carbon dioxide in the air to form a Li_2CO_3 interface layer, which leads to a decline of its conductivity (Liu et al., 2018). The $Li_{1.3}Al_{0.3}Ti_{1.7}(PO_4)_3$ with a NASICON structure is synthesized (Ma et al., 2016), although its ion conductivity is found to be as high as 1.21×10^{-3} S/cm, it is unstable because it is in direct contact with lithium metal and side reactions will occur, the Ti^{4+} ions in the structure would be reduced during charge and discharge (Hou et al., 2020). The $Li_{0.36}La_{0.56}Ti_{0.97}Al_{0.03}O_3$ with perovskite structure is prepared which shows ion conductivity of 2.54×10^{-3} S/cm at room temperature (Morata-Orrantia et al., 2003). This type of material possesses high grain ion conductivity, but the total ion conductivity conductivity is low because of its low interface conductivity. Similarly, the material is unstable to lithium, and Ti^{4+} will be reduced after contact with lithium (Sun et al., 2018).

$LiTa_2PO_8$ (LTPO) is a new type solid-state lithium ion electrolyte material reported in the latest research, which has high bulk ionic conductivity and low grain boundary ion conductivity. It is found that the LTPO material have ultra-high ionic conductivity of 35.3 mS/cm and ultra-low activation energy of 0.16 eV at room temperature through theoretical calculations (Hussain et al., 2019). In addition, the resulting LTPO ceramic electrolyte synthesized by simple conventional solid-phase displays grains conductivity of 1.6×10^3 S/cm and total ion conductivity of 2.5×10^4 S/cm at room temperature (Kim et al., 2018), which exhibits good application prospects. The Arrhenius plots for the conductivity of the LTPO are shown that the bulk conductivity is about one order of magnitude higher than the grain boundary conductivity (Kim et al., 2018; Ishigaki et al., 2020). The hot-pressing sintering technology is used to synthesize LTPO solid electrolytes, which can effectively reduce the grain-boundary resistance and improve Li-ion conductivity of LTPO (Huang et al., 2020). However, the hot pressing

sintering technology needs to increase the carbon removal process, which increases the risk of lithium carbonate on the surface of LTPO solid electrolytes. Previous studies found that excess lithium can improve the grain boundary conductivity of the material by adding excess lithium (Chung and Kang, 2014). In the garnet structure, the excess Li_2O formed a glassy phase at the grain boundary by adding excess lithium, which can eliminate residual pores and improve density (Li et al., 2013). In the perovskite structure, the effect of excessive lithium on the modification of grain boundaries is very important (Kwon et al., 2017). The reason is that the lithium on the grain boundaries is more volatile than the lithium in the crystal grains, and the amount of volatilization is uncertain (Wang et al., 2020). Therefore, it is necessary to actively explore the mechanism of lithium excess of electrolyte to improve the performance of all-solid-state electrolytes. Herein, in this work, the LTPO electrolyte is synthesized by high-temperature solid-phase method to compensate for uncontrollable lithium volatilization by adding excess lithium, while improving the microstructure of the material at grain boundaries. The results indicate that an excessive amount of Li_2O does not increase other impurities and change the structure of the material, but the liquid phase produced by the excess Li_2O can promote the elimination of interfacial pores, accelerate the direct bonding of grains and improve the ionic conductivity of grain boundary, thus improving the overall ionic conductivity of the material.

EXPERIMENTS

Synthesis and Preparation

The LTPO electrolyte was synthesized by conventional solid-phase reaction. according to the formula $LiTa_2PO_8+ xLi_2O$ (x = 0, 10, 20, 30, and 40 wt%), and corresponding excess Li_2CO_3 (99.5%, AR), Ta_2O_5 (99.5%, AR), and $(NH_4)_2HPO_4$ (99.5%, AR) according to the stoichiometry of the chemical formula is used as a raw material. The mixed powders were ball-milled for 12 h, and heated at 650°C for 4 h, to complete the thermal decomposition process. After the obtained powder was milled in an alumina crucible and ball milled again for 12 h, it was dried and heated at 950°C for 12 h via heat treatment process to complete the solid-state reaction. After the product was milled and dried, 0.6 g of the obtained powder was added to a mold (Φ10 mm) a pressure of 800 Mpa in the form of cold isostatic pressing was applied on the mold, to obtain the ceramic body with size of Φ10 mm × 1 ± 0.02 mm. The ceramic electrolyte sample was obtained by burying the powder of ceramic green embryo at 1050°C for 12 h.

Characterization Techniques

X-ray diffraction (XRD) patterns were performed at room temperature on the Rigaku-MiniFlex600 X-ray diffractometer using a Cu-Ka1 radiation, with operating voltage of 40 Kv and operating current of 15 mA. The data was collected at room temperature with a step size of 0.02 degrees and scan angle range of 10–50°. A scanning electron microscope (Zeiss Crossbeam 340 type) was used to characterize the microstructure

of the fractured ceramic electrolyte specimen surface. OHAUS-AX124ZH/E densitometer was used to test the density of the sample using Archimedes drainage method in anhydrous ethanol medium. The lithium ionic conductivity of LTPO ceramic electrolyte specimen were measured by Autolab ChemStation in a wide frequency range of 0.1–1 MHz with a amplitude of 10 mV, and the test data was fitted with Z-View impedance software. The ion conductivity was tested and calculated at different temperatures through the formula $\sigma = \frac{L}{R \cdot S}$, where σ is the ion conductivity, L is the sample thickness, R is the impedance value of the fitted equivalent circuit, and S is the measurement surface area of the sample. the activation energy of the ion was calculated through the Arrhenius equation $\sigma T = A\exp(-\frac{E_\alpha}{kT})$, where E_α is the activation energy of the sample, and A, k, and T are the pre-exponential factor, Boltzmann's constant and absolute temperature, respectively. The surface hardness of LTPO ceramic electrolyte specimen was measured using the Shanghai Fall of – HV5 type nanoindenter, a pressure of 1 kg was applied and staying for 10 s, and an average value of surface hardness was obtained by measuring six times. An electrochemical cycle test of the LTPO ceramic electrolyte specimen was performed. Before the test, a vacuum sputtering method was used to sputter gold electrodes on the polished surface of the sample. The cyclic voltammetry curves (CV) were evaluated by IVIUMnSTAT electrochemical workstation, with scanning speed of 0.5 mV s^{-1} and scanning voltage range of -0.5

to 5 V. The X-ray photoelectron spectroscopy (XPS) experiments were performed using a Thermo Scientific^{TM} K-Alpha X-ray photoelectron spectrometer with a monochromatic Al Kα X-ray source. Before testing, the samples were dried in vacuum for 24 h.

RESULTS AND DISCUSSION

Figure 1 shows the XRD patterns of LTPO electrolytes with different lithium additions sintered at a temperature of 1050°C for 12 h. From the XRD diffraction spectrum analysis, it is found that with the increase of Li content in the sample, the main crystal phase of the synthetic material is still consistent with the LTPO reported in the literature (Kim et al., 2018; Huang et al., 2020; Ishigaki et al., 2020). However, with the increase of lithium content, the phase of $LiTa_3O_8$ gradually appeared in the test results, especially when the content of added excess lithium was 40 wt%, the phase of $LiTa_3O_8$ appeared obvious diffraction peaks. It shows that excessive lithium leads to the dissolution of Ta^{5+} ions in the structure and the formation of a dielectric phase, which is unfavorable to the improvement of the ionic conductivity of the LTPO material. Comparing the peak diffraction data (**Table 1**) of the materials obtained with different lithium additions, it is found that the sample with lithium content over 20 wt% has the best crystallization performance. From the diffraction
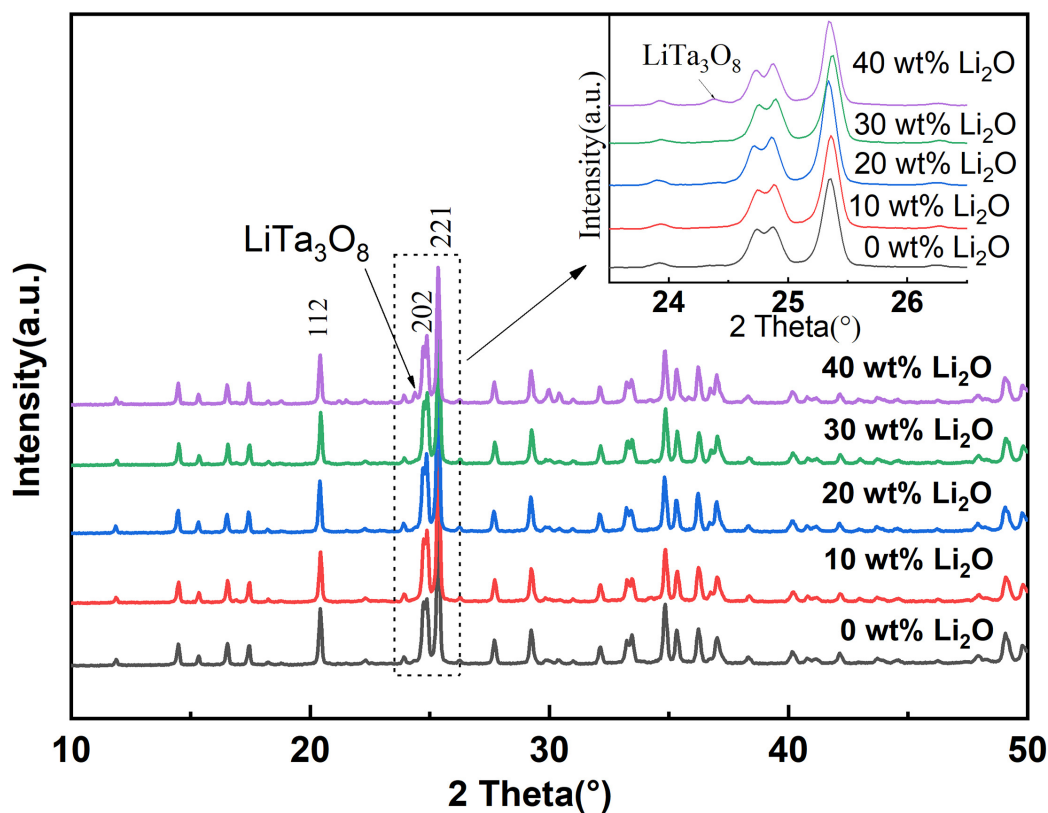

FIGURE 1 | Powder XRD patterns of LTPO prepared with different excess lithium addition amount sintered at 1050°C for 12 h.

TABLE 1 | The partial interplanar spacing of different Li_2O excess LTPO obtained from XRD.

Excess lithium (wt%)	Interplanar spacing (Å)		
	(112)	**(202)**	**(221)**
0	4.3454	3.5760	3.5093
10	4.3455	3.5759	3.5116
20	4.3495	3.5785	3.5118
30	4.3422	3.5755	3.5091
40	4.3495	3.5783	3.5120

data, the interplanar spacing was calculated, and found that the crystal interplanar spacing of the obtained samples has a certain difference with the amount of lithium added. The appropriate amount of lithium can increase the interplanar spacing, but the overcoming lithium addition creates new materials phase.

Figure 2 shows the scanning electron micrographs (SEM) of the samples obtained with different excess lithium content, and the density and surface hardness of the samples. For the sample with 0 wt% Li excess (**Figure 2a**), it is found that the grains of LTPO ceramics sintered at 1050°C for 12 h are mostly elongated, with a length of 1–2 μm and a width of about 0.5 μm, and there are some pores between grains. As the lithium content increases to 10 wt% (**Figure 2b**), it is found that the voids in the sample are decreasing, indicating that the liquid phase formed by the presence of excess lithium is beneficial to the discharge of gas. At the same time, under the action of the liquid phase, the binding between the particles is closer. For the sample with 20 wt% lithium excess (**Figure 2c**), the effect is more obvious, the particles are packed tighter, and the cohesive effect of the liquid phase is more obvious. For the sample with an excess lithium

content of more than 30 wt% (**Figure 2d**), it is found that a small amount of new phases are generated at the grain boundaries, and some small spherical grains with a diameter of about 0.5–1 μm appeared. Based on the XRD data, we speculate that when the lithium content increases, Ta^{5+} in $LiTa_2PO_8$ is dissolved out and reacts with excess lithium to produce $LiTa_3O_8$ crystal phase. As the amount of lithium continues to increase, the content of this new substance is increasing. When the lithium excess is 40 wt% (**Figure 2e**), the $LiTa_3O_8$ phase can already be distinguished by XRD patterns. In terms of density and hardness, it is also found that with the increase of excess lithium, the density and hardness increase first and then decrease (**Figure 2f** and **Table 2**). When the lithium content in the sample exceeds 20 wt%, the density and hardness reach the maximum. This indicates that as the lithium content increases, lithium begins to act as a binder. As the lithium excess continues, the sample effect reaches the maximum when the lithium excess is 20 wt%. With the continuous increase of lithium, the second phase of $LiTa_3O_8$ at the $LiTa_2PO_8$ interface is produced, and the density of the particles and the hardness of the sample are reduced.

The AC impedance spectra of samples with different amounts of lithium are tested, and the results are shown in **Figure 3**. Z-view fitting software is used to fit the impedance data at a frequency of 0.1–1 MHz, and the Arrhenius equation is used to calculate the ion conductivity. it is found that according to the normal chemical formula ratio, the conductivity of the grain boundary sample is 3.41×10^{-5} S/cm, which is far from the theoretically calculated conductivity in the literature. When the lithium oxide content exceeds 20%, the excess lithium oxide increases the liquid phase content during the sintering process, and enhances the liquid phase adhesion. As a result, the grain boundary conductivity begins to increase, which is 3.28×10^{-4} S/cm. This conductivity is about ten times that of lithium without excess, which indicates that excessive lithium has

FIGURE 2 | SEM, density, and hardness under different lithium additions, **(a–f)** are represented as 0, 10, 20, 30, 40 wt%, and density, hardness graph.
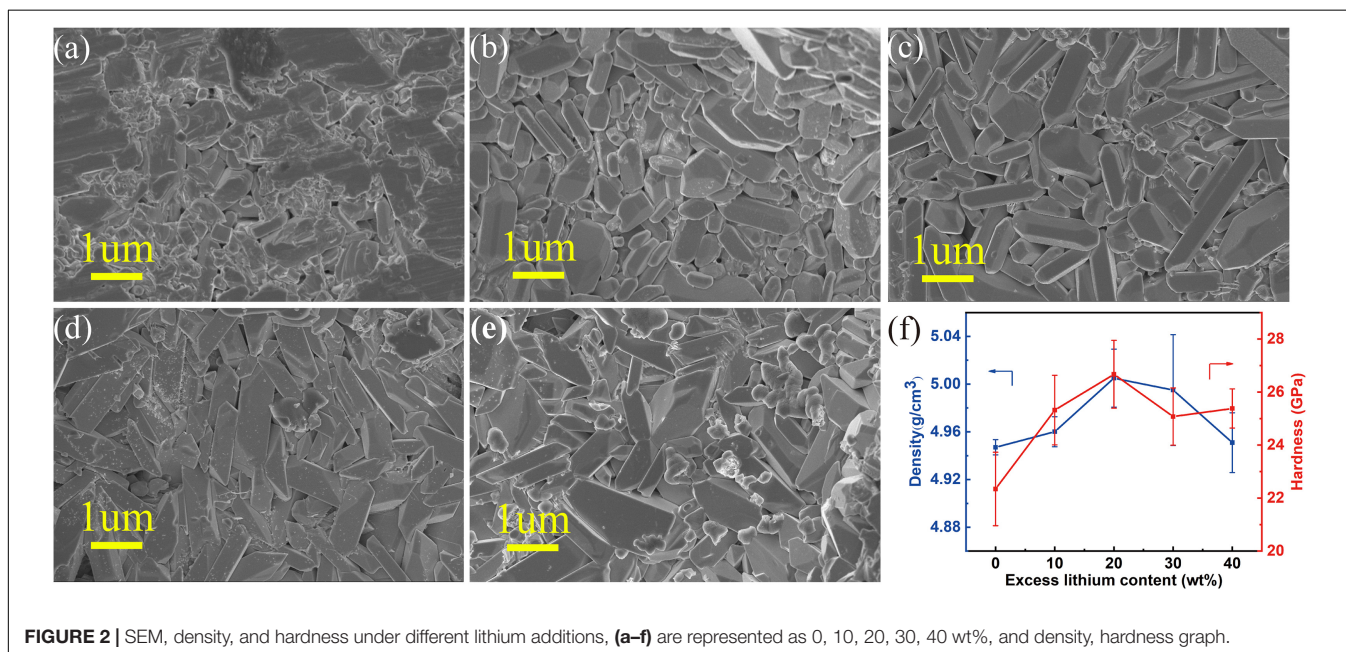
TABLE 2 | Density, surface hardness, electrical conductivity, and activation energy of LTPO with different excess lithium content.

Excess lithium (wt%)	Density ρ (g/cm³)	Relative density (%)	Hardness (GPa)	Total conductivity σ (S/cm)	Activation energy (Ev)
0	4.9470	84.59	22.3445	3.41×10^{-5}	0.41
10	4.9601	84.82	25.3188	6.99×10^{-5}	0.34
20	5.0050	85.58	26.6704	3.28×10^{-4}	0.27
30	4.9950	85.41	25.0756	2.49×10^{-4}	0.33
40	4.9509	84.66	25.3802	1.97×10^{-4}	0.34
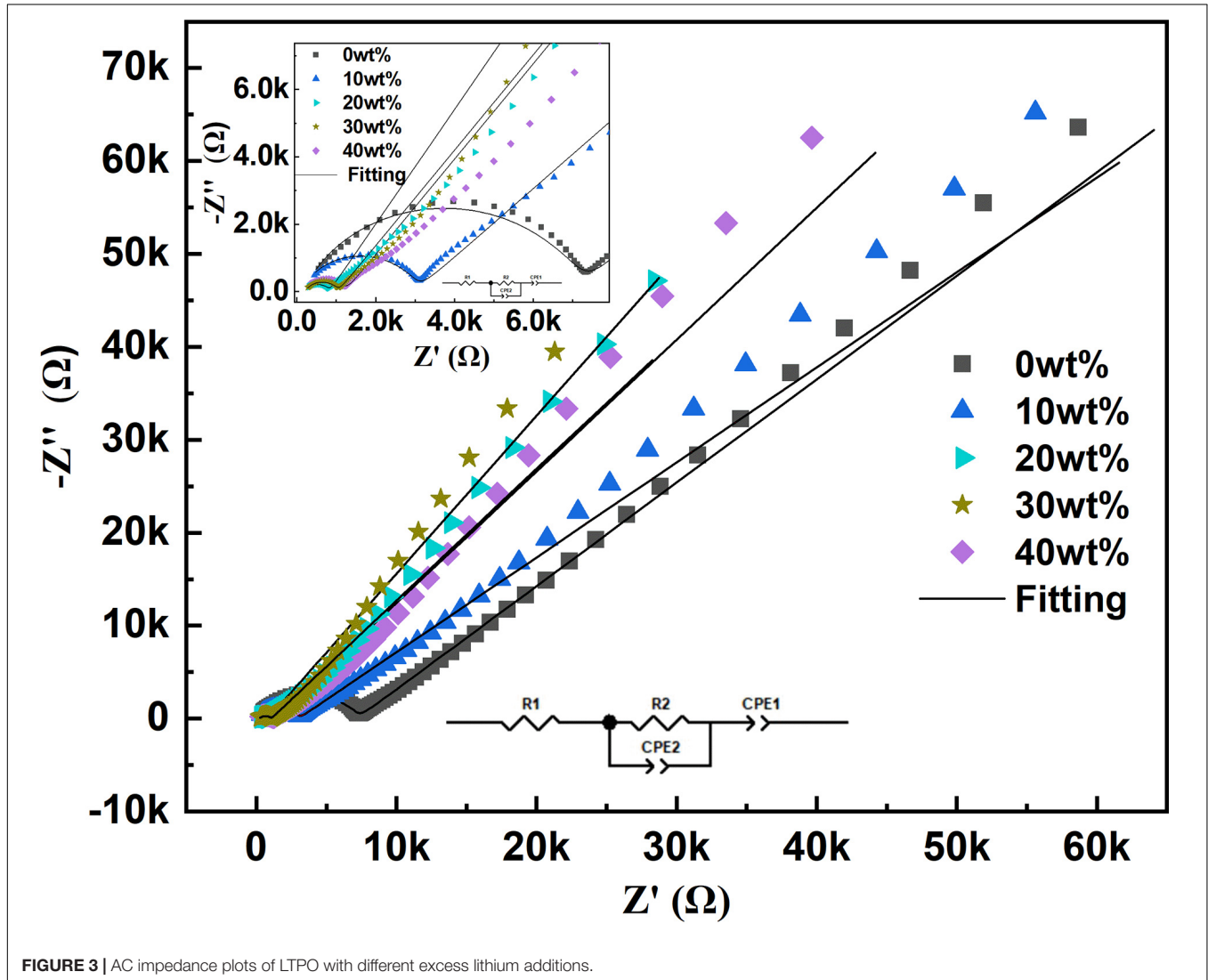
FIGURE 3 | AC impedance plots of LTPO with different excess lithium additions.

a significant effect on improving the ionic conductivity of the sample. However, as the lithium content continues to increase, the conductivity still shows a downward trend. When the lithium excess in the sample is 40 wt%, the ionic conductivity decreases by 1.97×10^{-4} S/cm. This is because excess lithium induces the formation of $LiTa_3O_8$ grains, which hinder the transport of ions.

As shown in **Figure 4**, a similar correspondence is observed accordingly for the change of activation energy. With an excess of 20 wt% lithium, the activation energy can reach 0.27 eV; as the excess lithium continues to increase, the activation also continues

to increase. The existing research data shows that $LiTa_3O_8$ is a kind of dielectric phase, which is not conducive to the conduction of lithium ions.

In order to verify the application of LTPO electrolyte in all-solid-state batteries, Li| LTPO| Li symmetric batteries were fabricated and tested. In a symmetrical battery without any other electrolyte composition, the metal lithium on both sides of the LTPO ceramic is in contact with each other through pressure, and the charge and discharge test is performed at 30°C. In order to explore the limit current density of the battery, the battery
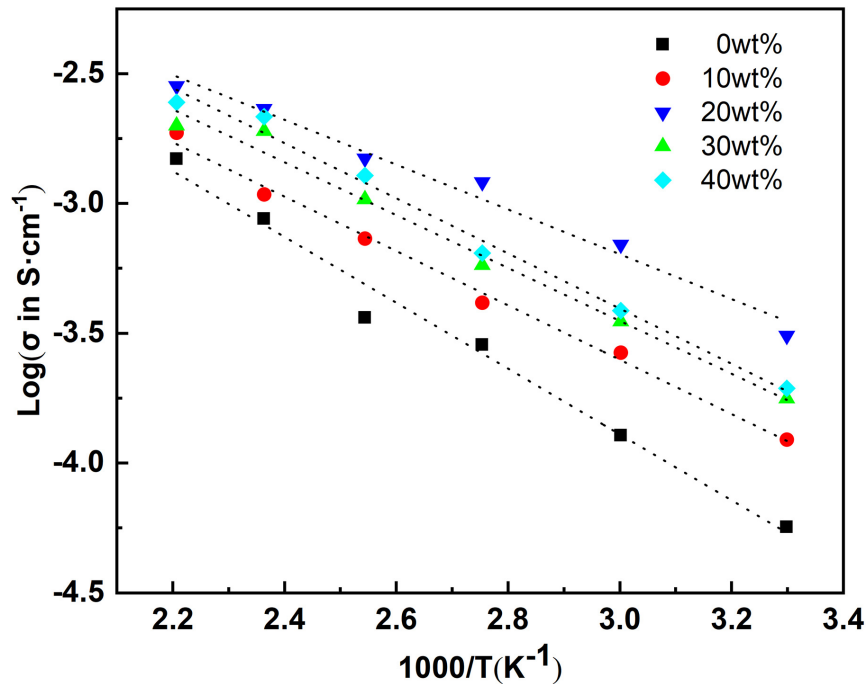
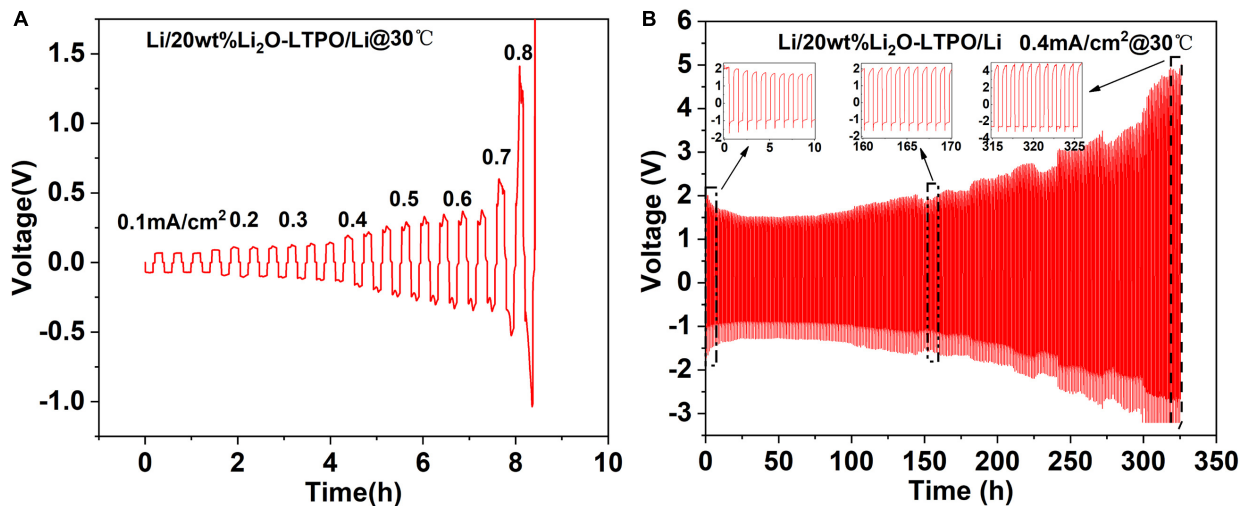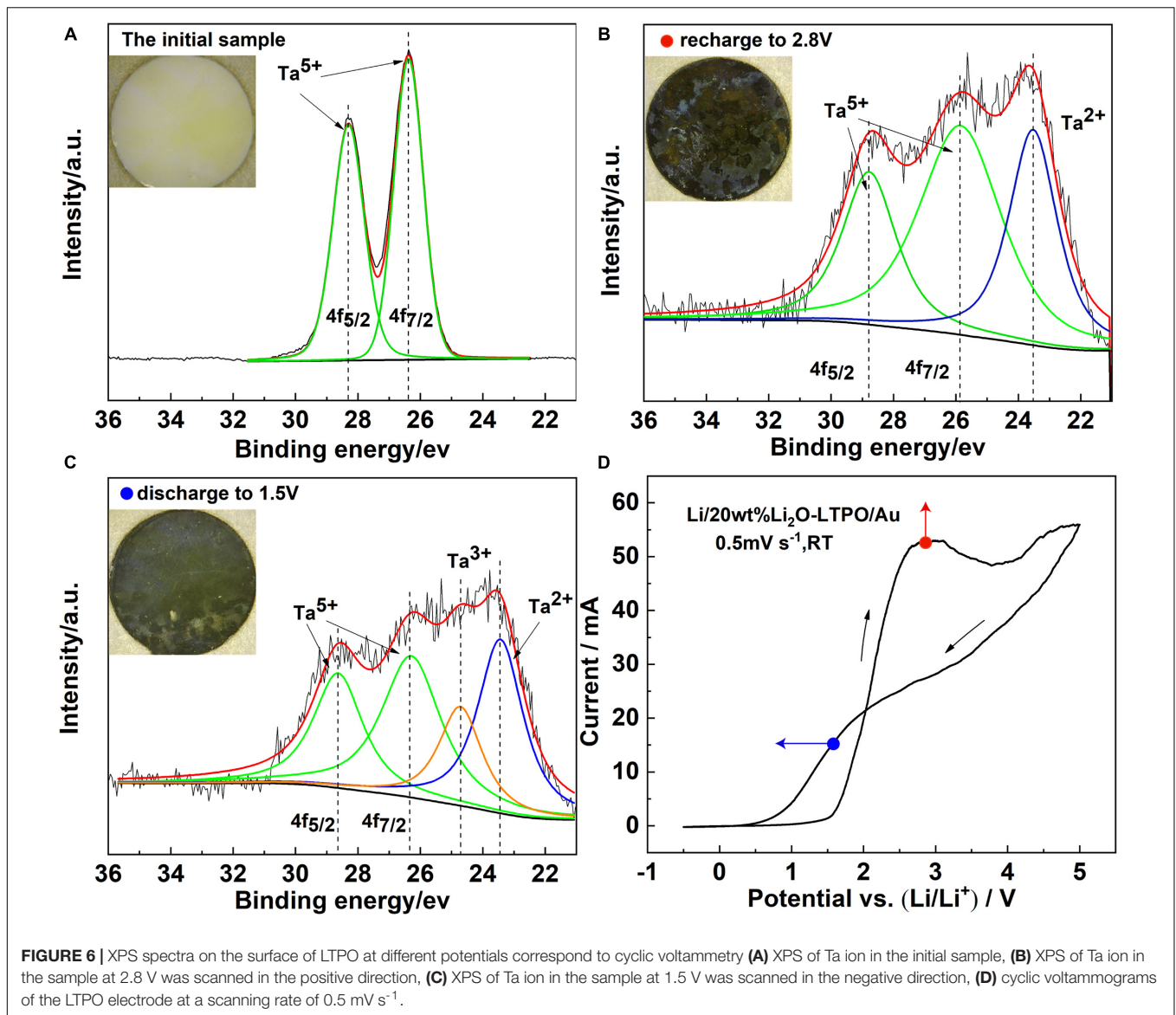**FIGURE 4 |** Arrhenius plots of the LTPO samples in the temperature range of 303–453 K.

FIGURE 5 | (A) Galvanostatic cycling performance of the Li| LTPO| Li symmetric cell at different current densities **(B)** 0.4 mA/cm^2 cycle stability of the ceramic electrolyte specimen.

was tested under different charge and discharge current densities. The results show that as the test current density increases, the polarization voltage of the battery gradually rises (**Figure 5**). It can be found when the battery charge/discharge current density returned to 0.4 mA/cm^2, the battery has a polarization potential of up to 2 V, and the polarization potential continues to increase as the charge and discharge cycle goes on. This shows that there is a large interface impedance between the electrolyte sheet and the metal lithium, as a result, the interface impedance continues

to increase with the progress of the electrochemical reaction, the contact interface continues to grow, and the contact interface between LTPO and metal lithium is unstable.

In order to further verify the instability of contact between LTPO and lithium metal, a cyclic voltammogram of a cell with LTPO as the cathode and Li metal as the anode was performed at a scanning rate of 0.5 mV s^{-1} and the XPS spectra on the surface of the electrolyte sheet were investigated as shown in **Figure 6**. It can be seen that there is an oxidation potential at about 2.8 V,

FIGURE 6 | XPS spectra on the surface of LTPO at different potentials correspond to cyclic voltammetry **(A)** XPS of Ta ion in the initial sample, **(B)** XPS of Ta ion in the sample at 2.8 V was scanned in the positive direction, **(C)** XPS of Ta ion in the sample at 1.5 V was scanned in the negative direction, **(D)** cyclic voltammograms of the LTPO electrode at a scanning rate of 0.5 mV s^{-1}.

corresponding to a reduction potential of 1.5 V, which indicates that the electrolyte material has a redox reaction in this process, and the LTPO material is unstable when contacting with lithium in the voltage range of 0.5–5 V, and redox will occur, but this process is reversible.

As shown in **Figure 6A**, LTPO material without contact with lithium has two characteristic peaks at the binding energy of 26.43 and 28.28 eV in the 4F high-resolution spectrum of Ta, and the spin-splitting orbital is 1.9 eV, which is very consistent with the characteristic peaks of Ta $4F_{7/2}$ and Ta $4F_{5/2}$ of Ta^{5+}. It can be seen that there is an oxidation potential at about 2.8 V, corresponding to a reduction potential of 1.5 V, which indicates that the electrolyte material has a redox reaction in this process, and the LTPO material is unstable when contacting with lithium in the voltage range of 0.5–5 V, and redox will occur, but this process is reversible. the symmetrical battery samples kept at 1.5 and 2.8 V were disassembled, however, after contact with

lithium, the XPS spectrum line changes under the action of 2.8 V (**Figure 6B**), Ta^{5+} ions are reduced, and the characteristic peak of Ta^{2+} appears. When the voltage is further reduced to 1.5 V (**Figure 6C**), the content of Ta^{2+} ions increases, and the reduction of Ta^{5+} becomes more serious. Therefore, it can be concluded that direct contact with lithium metal should be avoided when using LTPO material as solid electrolyte.

CONCLUSION

In this work, the addition of excessive lithium in the process of LTPO material synthesis can effectively increase its lithium ion conductivity, and can effectively compensate for the lithium evaporation during the sintering process. At the same time, the liquid phase can effectively promote the completion of the sintering process. The discharge of the pores increases the

adhesion between the crystal grains and reduces the interface resistance of the material. When the lithium excess is 20 wt%, the best ionic conductivity and ion activation energy at room temperature can be observed. However, if the lithium content continues to increase, the resulting liquid phase can dissolve the Ta^{5+} in the structure, and produce a $LiTa_3O_8$ crystal phase with dielectric properties at the grain boundary, which will hinder the transport of lithium ions. In addition, the LTPO material is unstable in direct contact with metallic lithium and can be reduced by metallic lithium, which will be an important issue to be addressed for the LTPO solid state electrolytes in the future.

DATA AVAILABILITY STATEMENT

The original contributions presented in the study are included in the article/supplementary material, further inquiries can be directed to the corresponding author/s.

REFERENCES

Muench, S., Wild, A., Friebe, C., Haupler, B., Janoschka, T., and Schubert, U. S. (2016). Polymer-based organic batteries. *Chem. Rev.* 116, 9438–9484. doi: 10.1021/acs.chemrev.6b00070

Zhou, D., Shanmukaraj, D., Tkacheva, A., Armand, M., and Wang, G. (2019). polymer electrolytes for lithium-based batteries: advances and prospects. *Chem* 5, 2326–2352. doi: 10.1016/j.chempr.2019.05.009

Long, L., Wang, S., Xiao, M., and Meng, Y. (2016). Polymer electrolytes for lithium polymer batteries. *J. Mater. Chem. A* 4, 10038–10069. doi: 10.1039/c6ta02621d

Kato, Y., Hori, S., Saito, T., Suzuki, K., Hirayama, M., Mitsui, A., et al. (2016). High-power all-solid-state batteries using sulfide superionic conductors. *Nat. Energy* 1:16030. doi: 10.1038/nenergy.2016.30

Dong, Z., Xu, C., Wu, Y., Tang, W., Song, S., Yao, J., et al. (2019). Dual substitution and spark plasma sintering to improve ionic conductivity of garnet Li7la3zr2o12. *Nanomaterials* 9:721. doi: 10.3390/nano9050721

Liu, Q., Geng, Z., Han, C., Fu, Y., Li, S., He, Y.-b., et al. (2018). Challenges and perspectives of garnet solid electrolytes for all solid-state lithium batteries. *J. Power Sources* 389, 120–134. doi: 10.1016/j.jpowsour.2018.04.019

Ma, F., Zhao, E., Zhu, S., Yan, W., Sun, D., Jin, Y., et al. (2016). Preparation and evaluation of high lithium ion conductivity Li 1.3 Al 0.3 Ti 1.7 (PO 4) 3 solid electrolyte obtained using a new solution method. *Solid State Ion.* 295, 7–12. doi: 10.1016/j.ssi.2016.07.010

Hou, M., Liang, F., Chen, K., Dai, Y., and Xue, D. (2020). Challenges and perspectives of NASICON-type solid electrolytes for all-solid-state lithium batteries. *Nanotechnology* 31:132003. doi: 10.1088/1361-6528/ab5be7

Morata-Orrantia, A., García-Martín, S., and Alario-Franco, M. Á. (2003). Optimization of lithium conductivity in La/Li titanates. *Chem. Mate.* 15, 3991–3995. doi: 10.1021/cm0300563

Sun, Y., Guan, P., Liu, Y., Xu, H., Li, S., and Chu, D. (2018). Recent progress in lithium lanthanum titanate electrolyte towards all solid-state lithium ion secondary battery. *Crit. Rev. Solid State Mater. Sci.* 44, 265–282. doi: 10.1080/10408436.2018.1485551

Hussain, F., Li, P., and Li, Z. (2019). Theoretical insights into Li-ion transport in LiTa2PO8. *J. Phys. Chem. C* 123, 19282–19287. doi: 10.1021/acs.jpcc.9b03313

Kim, J., Kim, J., Avdeev, M., Yun, H., and Kim, S.-J. (2018). LiTa2PO8: a fast lithium-ion conductor with new framework structure. *J. Mater. Chem. A* 6, 22478–22482. doi: 10.1039/c8ta09170f

Ishigaki, N., Kataoka, K., Morikawa, D., Terauchi, M., Hayamizu, K., and Akimoto, J. (2020). Structural and Li-ion diffusion properties of lithium tantalum phosphate LiTa2PO8. *Solid State Ion.* 351:115314. doi: 10.1016/j.ssi.2020.115314

Huang, B., Xu, B., Zhang, J., Li, Z., Huang, Z., Li, Y. et al. (2020). Li-ion conductivity and stability of hot-pressed LiTa2PO8 solid electrolyte for all-solid-state batteries. *J. Mater. Sci.* 56, 2425–2434. doi: 10.1007/s10853-020-05324-9

Chung, H., and Kang, B. (2014). Increase in grain boundary ionic conductivity of Li1.5Al0.5Ge1.5(PO4)3 by adding excess lithium. *Solid State Ion.* 263, 125–130. doi: 10.1016/j.ssi.2014.05.016

Li, Y., Cao, Y., and Guo, X. (2013). Influence of lithium oxide additives on densification and ionic conductivity of garnet-type Li6.75La3Zr1.75Ta0.25O12 solid electrolytes. *Solid State Ion.* 253, 76–80. doi: 10.1016/j.ssi.2013.09.005

Kwon, W. J., Kim, H., Jung, K.-N., Cho, W., Kim, S. H., Lee, J.-W., et al. (2017). Enhanced Li+ conduction in perovskite Li3xLa2/3-x?1/3-2xTiO3 solid-electrolytes via microstructural engineering. *J. Mater. Chem. A* 5, 6257–6262. doi: 10.1039/c7ta00196g

Wang, C., Fu, K., Kammampata, S. P., McOwen, D. W., Samson, A. J., Zhang, L., et al. (2020). garnet-type solid-state electrolytes: materials, interfaces, and batteries. *Chem. Rev.* 120, 4257–4300. doi: 10.1021/acs.chemrev.9b00427